

PACS numbers: 42.60.By; 42.70.Hj; 42.65.Re; 42.65.Yj
DOI: 10.1070/QE2014v044n05ABEH015438

Multiterawatt femtosecond laser system with kilohertz pulse repetition rate

V.V. Petrov, E.V. Pestryakov, A.V. Laptev, V.A. Petrov, G.V. Kuptsov, V.I. Trunov, S.A. Frolov

Abstract. **The basic principles, layout and components are presented for a multiterawatt femtosecond laser system with a kilohertz pulse repetition rate *f*, based on their parametric amplification and laser amplification of picosecond radiation that pumps the stages of the parametric amplifier. The results of calculations for a step-by-step increase in the output power from the LBO crystal parametric amplifier channel up to the multiterawatt level are presented. By using the developed components in the pump channel of the laser system, the parameters of the regenerative amplifier with the output energy ~1 mJ at the wavelength 1030 nm and with *f* = 1 kHz are experimentally studied. The optical scheme of the diode-pumped multipass cryogenic Yb : Y_2O_3 laser ceramic amplifier is developed and its characteristics are determined that provide the output energy within the range 0.25–0.35 J.**

Keywords: *laser media, laser diode pumping, femtosecond pulses, high-intensity laser systems, cryogenic temperatures.*

1. Introduction

Recently, a particular attention has been paid to the development of principles and components of high-intensity femtosecond laser systems with multiterawatt power and pulse repetition rate at the kilohertz level. The main goal of these studies is to construct laser systems with the intensity reaching the ultrarelativistic limit (10^{25} W cm^{-2}), intended for studying the physics of extreme laser fields and performing experimental studies on nonlinear quantum electrodynamics, as well as for principally new technological applications, such as laser acceleration of charged particles, laser-assisted thermonuclear fusion, etc. [1, 2].

The studies show that the creation of such systems is most promising when use is made of parametric amplification of femtosecond pulses with the help of optical parametric chirped pulse amplification (OPCPA) [3], pumped by solid-state lasers, whose active media are excited by the radiation of laser diodes. In this connection, within the frameworks of such projects as LUCIA [4], DiPOLE [5], HiLASE [6] significant efforts were undertaken aimed at elaborating the components for diode-pumped solid-state laser systems, operating at pulse energies of 100 J and higher. The use of radiation produced by these systems for pumping optical parametric amplifiers (OPAs) will allow construction of femtosecond systems, having a multiterawatt and petawatt peak power with a high pulse repetition rate [3].

In spite of the active studies carried out in leading laser centres, the work in this field is still far from completion. The goal of our project is to develop this area on the basis of the components that use large-size nonlinear crystals, belonging to the borate group (BBO and LBO), in the channel of parametric amplification, and crystalline and ceramic laser-active elements from the group of aluminium garnets (YAG, LuAG) and sesquialteral oxides (Y_2O_3, Lu_2O_3, etc.) in the laser amplification channel for the radiation that pumps the OPA.

Within the framework of the project the following studies were carried out.

1. The principal scheme of step-by-step development of a femtosecond laser system from terawatt to multiterawatt peak powers, based on the use of the OPCPA channel of broadband OPA femtosecond pulses was developed. The OPA was pumped using the radiation from the chirped parametric amplification (CPA) channel of laser amplifiers based on diode-pumped optical crystalline and ceramic elements, doped with Yb ions, operating at room and cryogenic temperatures.

2. The numerical modelling of the OPCPA channel, parametrically amplifying the initial femtosecond radiation pulse having the bandwidth 300 nm at the centre wavelength 1030 nm up to the peak power 100 TW was carried out; the layout and optimal dimensions of the BBO and LBO nonlinear crystals were determined.

3. Pulse stretchers for the generator of initial femtosecond pulses in the OPCPA and CPA amplification channels were developed and studied.

4. The cryogenic operation regime of the Yb : KYW crystal regenerative amplifier in the CPA channel was experimentally studied.

5. The multipass amplifier in the CPA channel of laser amplification, based on the Yb:YAG, Yb:LuAG crystal and Yb : Y_2O_3, Yb : Lu_2O_3 ceramic elements, was modelled numerically.

V.V. Petrov, V.A. Petrov, G.V. Kuptsov Institute of Laser Physics, Siberian Branch, Russian Academy of Sciences, prosp. Akad. Lavrentyeva 13/3, 630090 Novosibirsk, Russia; Novosibirsk State Technical University, prosp. K. Marksa 20, 630073 Novosibirsk, Russia; e-mail: vpetv@laser.nsc.ru;
E.V. Pestryakov Institute of Laser Physics, Siberian Branch, Russian Academy of Sciences, prosp. Akad. Lavrentyeva 13/3, 630090 Novosibirsk, Russia; Novosibirsk National Research State University, ul. Pirogova 2, 630090 Novosibirsk, Russia; e-mail: pefvic@laser.nsc.ru;
A.V. Laptev, V.I. Trunov, S.A. Frolov Institute of Laser Physics, Siberian Branch, Russian Academy of Sciences, prosp. Akad. Lavrentyeva 13/3, 630090 Novosibirsk, Russia

Received 3 March 2014; revision received 11 March 2014
Kvantovaya Elektronika **44** (5) 452–457 (2014)
Translated by V.L. Derbov

2. Structure of a multiterawatt femtosecond laser system

The basic principle of the system construction is the broadband parametric OPCPA amplification of pulses from the starting femtosecond laser. The parametric amplifier is pumped by the second harmonic of a part of radiation from the same starting laser, CPA-amplified in diode-pumped laser crystal and ceramic elements doped with Yb^{3+} ions. The radiation from the starting femtosecond oscillator with the centre wavelength 1030 nm is divided and amplified in two channels, the CPA channel forming the picosecond radiation for OPA pumping, and the OPCPA channel of parametric amplification, which simplifies the implementation of optical synchronisation of channels.

The CPA pump channel includes a stretcher, a regenerative amplifier, a multipass amplifier, a compressor and a frequency-doubling (SHG) unit based on a nonlinear crystal from the borate group.

The OPCPA amplification channel consists of a segment of photonic-crystal fibre (PCF), intended for enrichment of the spectrum of radiation generated by the starting femtosecond Yb laser, and forming the pulses with the duration of 10–11 fs at the output of the system after amplification, a negative stretcher, a sequence of OPA stages on the basis of nonlinear-optical crystals from the borate group, and compressors based on chirped mirrors and positive-dispersion optical materials. All this allows step-by-step development of the system from terawatt to multiterawatt and even petawatt peak powers.

It is also worth noting that the use of novel laser materials, doped with Yb^{3+} ions, offers an opportunity to obtain high-power pulses of picosecond duration in the pump channel at the expense of sufficiently large gains at cryogenic temperatures of the active media and diode pumping, the use of which reduces the influence of thermal effects on the active elements and allows an increase in the pulse repetition rate up to a kilohertz level.

To implement the step-by-step development of the femtosecond laser system, presented in Fig. 1, we numerically modelled the parametric amplification channel and determined the radiation parameters that provide a step-by-step growth of peak powers at the output of the system from terawatt to multiterawatt level by increasing the number of stages in the OPCPA channel. The modelling was implemented using the split-step method [7]. In the calculations the influence of linear and nonlinear phase effects on the parametric amplification of femtosecond pulses with picosecond pumping, the diffraction that determines the divergence of the beams, the walk-off of the radiation as a result of birefringence, the self-phase modulation and cross-modulation, as well as the small-scale self-focusing were taken into account.

Particular attention in the analysis of parametric amplification of spectrally broadband pulses was paid to the choice of nonlinear-optical crystals with extremely low absorption, both in the region of the gain spectrum of the signal frequencies and in the region of the idler frequency spectrum, simultaneously possessing high nonlinearity coefficients, peak intensities of the optical breakdown, and the amplification spectral widths at the given gain.

In our case these conditions are better satisfied by the LBO crystals that have the absorption $\sim 10^{-4}$ cm^{-1} in the range 800–1400 nm and provide the gain spectral width, sufficient to support the amplification of pulses with the duration smaller than 10 fs. As compared to the DKDP crystals, widely used in parametric amplifiers of high-power laser systems, the LBO crystals are characterised by greater nonlinearity coefficients and greater thresholds of optical breakdown ($\sim$20 GW cm^{-2}). The power gain of the LBO crystal is almost 3 times higher, the heat conductivity is 1.7 times greater, and the absorption coefficient in the region of the gain spectrum of the initial femtosecond pulses with the centre wavelength 1030 nm is almost by an order of magnitude lower than in the DKDP crystals.

The calculations have shown that in order to increase the output peak power step-by-step from 1 to 100 TW, the spectral bandwidth of the initial femtosecond radiation being $\sim$300 nm, with the spatial and temporal Gaussian profiles of the pulses with the duration $\sim$5 fs and the energy 1 nJ, the layouts presented in Fig. 2 should be used. The terawatt level of power is attained in the case of double-pass scheme with one 5×5×10 mm LBO crystal (Fig. 2a), and to obtain the multiterawatt power level (from 10 to 100 TW) one should use the double-crystal layouts (Fig. 2b).

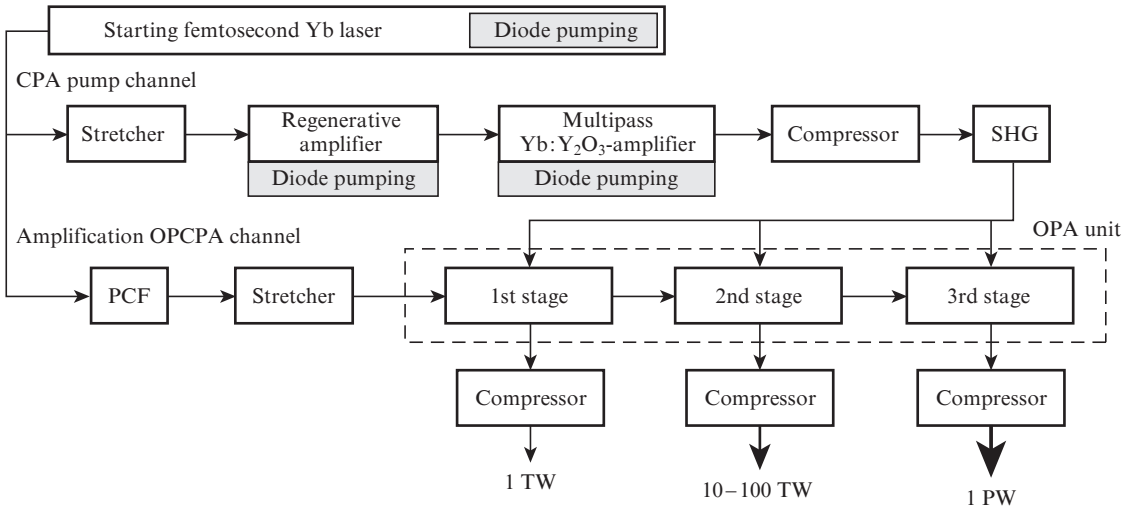

Figure 1. Schematic diagram of the multiterawatt femtosecond laser system with a pulse repetition rate up to 1 kHz.

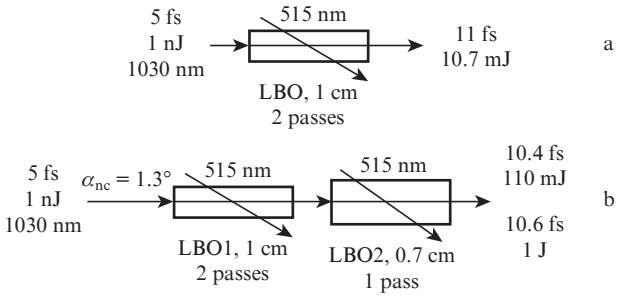

Figure 2. Schematic diagrams of the parametric amplification stages for achieving the powers (a) 1 TW and (b) 10 and 100 TW.

Table 1. Parameters of the stages of the OPCPA amplification channel.

Parameter	Output power of the stage/TW		
	1	10	100
Number of crystals	1	2	2
Number of passes through the first crystal 1 cm long	2	2	2
Number of passes through the second crystal 0.7 cm long	–	1	1
Pump energy of the first crystal/mJ	60	6	60
Pump energy of the second crystal/mJ	–	500	5000
Energy of amplified pulses/mJ	10.7	110	1000
Duration of amplified pulses/fs	11	10.4	10.6

The results of the numerical modelling of the OPCPA channel of parametric amplification of the pump radiation intensity for the crystals being no greater than 8 GW cm^{-2} are presented in Table 1. For each stage the following parameters were optimised: the ratio of the duration of the chirped amplified pulse to the duration of the pump pulse, the relative delay between these pulses, the angles of canting and the angles of synchronism, as well as the length of the crystals. In all cases the pumping was implemented using the 15-ps radiation pulses with a Gaussian profile in time and fourth-order hyper-Gaussian profile in space, the wavelength 515 nm, and the angle of canting $\alpha_{nc} = 1.3°$.

The number of stages in the layout is optimal for obtaining the maximal energy of the amplified pulses, keeping their duration within the range 10–11 fs. Figure 3 presents the calculated spectra of the initial and amplified pulses at each stage of amplification and the spectra of the amplified and idler wave at the output of the system for the amplification up to a multiterawatt level.

The calculations have shown that in order to reach the petawatt level of the system output power (1 PW, 10.4 fs, 11 J) the layout designed for 10 TW should be completed with the third single-pass LBO crystal stage 0.7 cm long, and the pump energy should be increased up to 50 J. The aperture of the LBO crystal units should be increased up to 100 mm.

3. Generator of starting femtosecond pulses and OPCPA channel of parametric amplification

As an active element in the starting femtosecond Yb laser system we used the 1.5-mm-thick Yb:Y_2O_3 laser ceramics (10 at. %) placed in the vacuum cryostat with Brewster windows [8]. The cavity was designed following the X-type four-mirror scheme with additional focusing onto the semiconductor saturable

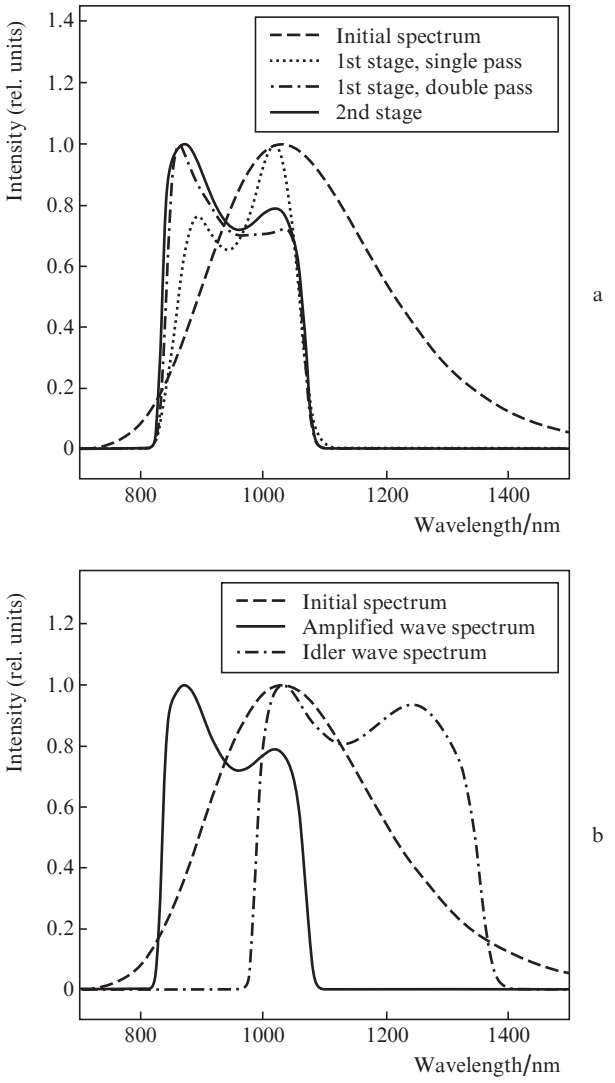

Figure 3. Spectra of the amplified pulses for the laser system with the power 100 TW: (a) for the amplified wave as a function of the number of passes and (b) for the amplified and idler waves at the output of the system.

absorber mirror (SESAM). The pump radiation (diode laser, 6 W, 975 nm) was focused through the corner mirror of the cavity with the curvature radius 100 mm into a spot with the diameter ~170 μm, coincident with the dimension of the cavity mode. The mode-locking regime was provided by the SESAM (the modulation depth 1.2%, the saturation energy density 70 μJ cm^{-2}, the relaxation time 500 fs, the group velocity dispersion –50 fs^2). The duration of output pulses at the centre wavelength 1030 nm amounted to ~300 fs, their repetition rate being 68.8 MHz.

The radiation from the starting Yb laser in the channel of parametric amplification passed through the segment of a SC-5.0-1040 photonic crystal fibre (NKT Photonics, NA = 0.20, the core diameter 4.8 μm, the nonlinear coefficient 11.5 W^{-1} km^{-1}), providing nonlinear transformation of the pulse and broadening of its spectrum. The increase in the spectral bandwidth of the initial radiation by ten times was achieved, which was sufficient to produce the pulses as short as ~10 fs [9].

After passing through the stretcher that increased its duration up to 10 ps the pulse arrived at the first parametric amplifier. The increase in the pulse duration in the stretcher was imple-

mented by means of two diffraction gratings (300 grooves mm^{-1}, the angle of incidence on the first grating 15°) [10]. The beam diameter and the size of the second diffraction grating (10^5 cm) determined the transmission bandwidth of the stretcher.

To compensate for the phase distortions, introduced by the photonic crystal fibre in the amplification channel, the stretcher, and the elements of the parametric amplifier, and to form a pulse with the duration 10 fs at the output of the system, the compressor of the amplification channel compensated for the chirp of the second, third and fourth order with the accuracy 12 fs^2, 730 fs^3, and 8500 fs^4, respectively [9].

4. CPA channel for pumping the parametric amplifiers

In the CPA pump channel of the parametric amplifiers of the laser system the pulse from the master $Yb:Y_2O_3$ laser was broadened from 250 fs to 1 ns using the double-pass stretcher, based on two parallel holographic diffraction gratings (1700 grooves mm^{-1}, the order of diffraction $m = -1$) and a spherical mirror with golden coating ($R = 1.52$ m) [10].

The values of the quadratic chirp after double passing through the stretcher and the regenerative amplifier (which corresponds to 100 passes through a 2-mm-thick element of the regenerative amplifier) amounted to 4.9×10^7 and 4×10^4 fs^2, respectively. The pump channel compressor reduced the pulse duration from 1 ns to 40 ps by means of two parallel diffraction gratings with the same number of grooves and the same angle of incidence on the first grating, as in the stretcher.

To raise the radiation power, the cryogenic Yb:KYW crystal regenerative amplifier (pulse repetition rate 1 kHz) was used in the pump CPA channel, increasing the radiation energy of the master oscillator from 1 nJ to 1 mJ.

The radiation, amplified in the cryogenic regenerative amplifier, had the following parameters: the pulse repetition rate ~70 MHz, the centre wavelength 1030 nm, the energy of the input pulse ~1 nJ, and the pulse duration not smaller than 250 ps. The energy gain amounted to $\sim10^6$. To match the positions and the diameters of the input beam and the fundamental mode in the cavity of the regenerative amplifier, the Galileo telescope with the transfer constant 0.9 was used. Figure 4 presents the dependence of the peak energy at the output of the regenerative amplifier on the power of the diode pump at the room and cryogenic temperature of the active medium. The experiments have shown that after cooling the crystal to the liquid nitrogen temperature and increasing the number of passes up to 100, the maximal peak energy at the output of the regenerative amplifier amounted to 700 μJ. A further increase in the pump power caused a breakdown of the optical coatings of the amplifier elements.

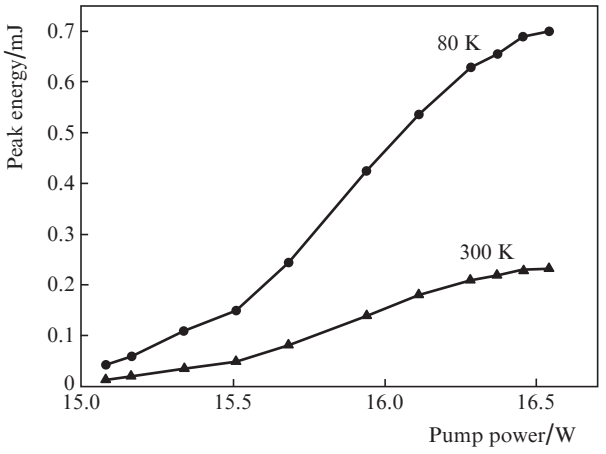

Figure 4. Peak energy at the output of the regenerative amplifier (1 kHz) vs. the pump power at the temperature of the active element 300 and 80 K.

In developing a multipass amplifier for the CPA pump channel of the system, a comparative analysis of physical properties of oxide ceramics and crystals ($Yb:Y_2O_3$, $Yb:Lu_2O_3$, Yb:YAG, and Yb:LuAG) (Table 2) has been carried out with the aim of choosing the most efficient active medium for operating at cryogenic temperatures with a high pulse repetition rate. The results of numerical modelling have shown the advantage of using the laser ceramics based on $Yb:Y_2O_3$ (Fig. 5). For this laser ceramics the influence of the radiation and pump beam profile on the output signal energy level was analysed, as well as the dependence of the output energy on the waist radius, of the output energy of the amplified signal on the incident power of pump [17], and of the small-signal gain on the energy absorbed in the active medium. The primary influence of the pump energy density and the active medium temperature on the gain and the efficiency of the amplifier operation were ascertained.

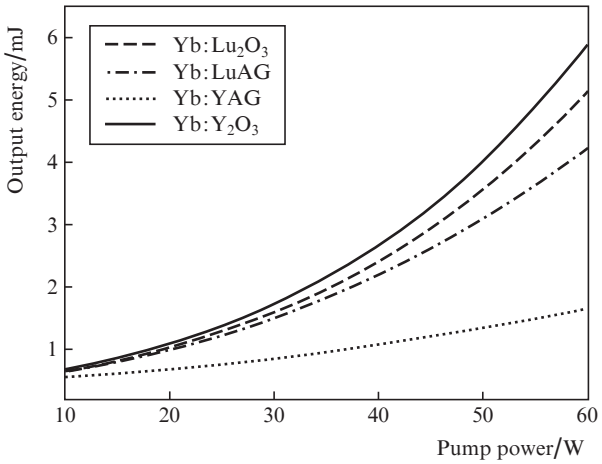

Figure 5. Dependence of the output energy of the amplified radiation on the pump power; the diameters of the pump and the amplified signal beam at the element are 0.5 mm.

To proceed to cryogenic temperatures, the gain cross-section of the $Yb:Y_2O_3$ ceramic active element was calculated and experimentally measured at room and cryogenic temperature (Fig. 6). The gain cross section was calculated based on the measured cross section of absorption σ_{ab} and emission σ_{em} using the following formula: $\sigma_g = \sigma_{ab}(1-\beta) + \sigma_{em}\beta$, where $\beta = N_1/(N_1 + N_2)$ is the ratio of the population of the upper laser energy level N_1 to the total population of the laser transition levels $N_1 + N_2$. In the cryogenic regime the gain cross section for the $Yb:Y_2O_3$ laser ceramics at the wavelength 1030 nm becomes three times as large as at room temperature.

The analysis of the calculated temperature dependence of the pump stored energy efficiency coefficient (the ratio of the energy stored in the element to the pump energy at the input of the active element) [18] has shown that the use of cryogenic temperatures increases the pump efficiency coefficient for the yttrium ceramics from 52% (at 300 K) to 65% (at 80 K).

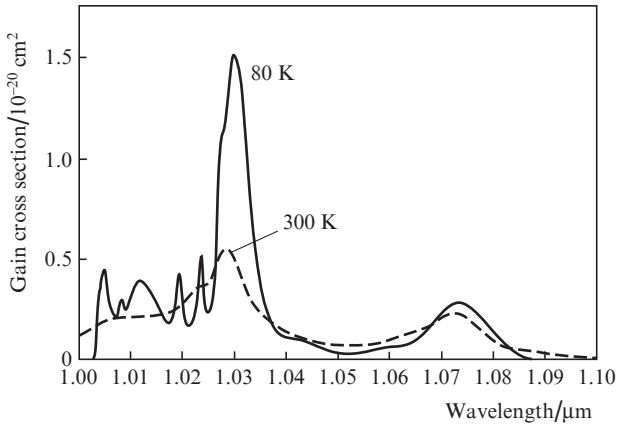

Figure 6. Gain cross section of the Yb:Y_2O_3 ceramic active element at $T = 300$ and 80 K for the parameter $\beta = 0.6$.

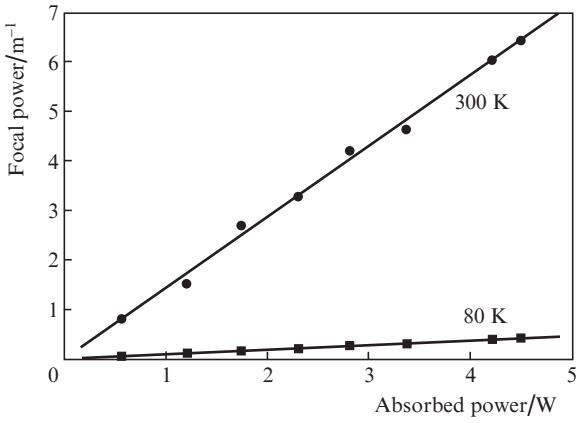

Figure 7. Dependence of the thermal lens focal power on the absorbed pump power in the Yb:Y_2O_3 laser ceramics at $T = 300$ and 80 K.

In order to determine the focal power of the thermal lens, the variation of the focal length was measured as a function of the absorbed diode pump power. The data presented in Table 2 show that the focal power of the thermal lens is changed by the value $D_{300}/D_{80} = 15.6$. The dependence of the focal power of the thermal lens on the absorbed pump power is presented in Fig. 7.

When the temperature reaches cryogenic values (80 K), the laser media doped with Yb^{3+} ions begin to operate according to the four-level scheme, which leads to a considerable growth of their efficiency and reduction of the active element thermal load.

To increase the efficiency and the output energy of the multipass amplifier up to 300–400 mJ the latter was structurally divided into two stages, the first of which was pumped by the diodes with the power up to 100 W, and the second one by the diodes of the kilowatt power level. For the first stage the optical scheme of a four-pass bow-tie Yb:Y_2O_3 ceramic amplifier was developed. The results of the calculations of the operation regimes for the first stage, obtained at the input energy 0.5 mJ and the diameters of the pumping and signal beams 1 mm, at room and cryogenic temperatures are presented in Fig. 8. It is necessary to note that the lowering of the first-stage active element temperature to 80 K leads to the reduction of the gain spectral width and the blue shift of the centre wavelength of the pulse by nearly 2 nm.

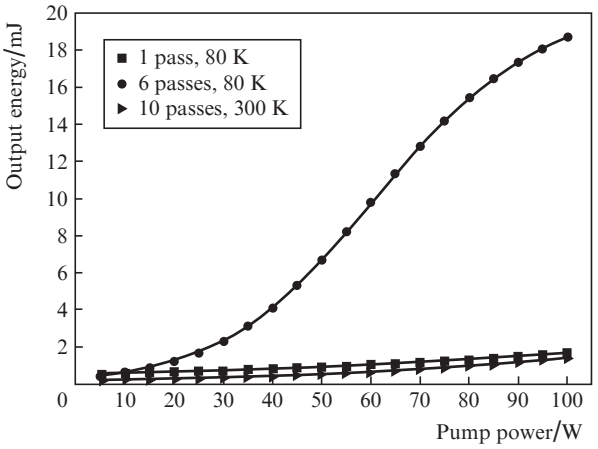

Figure 8. Dependence of the output energy of the radiation amplified by the first stage of the multipass amplifier on the pump power at the room and cryogenic temperature of the Yb:Y_2O_3 active element.

The operation of the second amplifier stage was analysed using the diode pumping with a kilowatt radiation power. Figure 9 shows the calculated dependence of the output radiation energy after amplifying in the second stage of the multipass

Table 2. Thermal and laser properties of the media, doped with ytterbium, at room and cryogenic temperatures.

Parameter	Active medium				
	Y_2O_3	Sc_2O_3	Lu_2O_3	YAG	LuAG
$\alpha_{300\,K}/10^{-6}$ K^{-1}	7.4 [12]	6.7 [12]	5.5 [12]	6.1 [12]	6 [11]
$\alpha_{123\,K}/10^{-6}$ K^{-1}	$1.5_{80\,K}$ [16]	2.3 [12]	2.9 [12]	2.9 [12]	–
$K_{300\,K}$/W m^{-1} K^{-1}	12.8 [11]	15.5 [11]	12.5 [11]	10.5 [11]	9 [11]
$K_{\sim 100\,K}$/W m^{-1} K^{-1}	$60_{80\,K}$ [16]	–	–	$38_{102\,K}$ [16]	–
$dn/dT_{270\,K}/10^{-6}$ K^{-1}	9 [12]	–21.4 [12]	8.18 [12]	10.16 [12]	8.3 [13]
$dn/dT_{90\,K}/10^{-6}$ K^{-1}	$2.3_{80\,K}$ [16]	–9.43 [12]	< –5.4 [12]	$0.9_{100\,K}$ [16]	–
$D^*_{300\,K}$/m^{-1} W^{-1}	1.42	3.2	–	1.2	–
$\sigma_{ab\ 300\,K}/10^{-20}$ cm^2 (λ_{ab}/nm)	2.4 [14] (976.7)	4.4 [14] (975.1)	3 [14] (976)	0.83 [14] (968.8)	0.67 [15] (969)
$\sigma_{em\ 300\,K}/10^{-20}$ cm^2	1 [14]	1.4 [14]	1.28 [14]	1.9 [14]	1.75 [15]
$\tau_{300\,K}$/ms	0.85 [14]	0.8 [14]	0.82 [14]	1 [14]	0.99 [15]
$\lambda_{em\ 300\,K}$/nm	1031 [14]	1041 [14]	1032 [14]	1030 [14]	1030 [15]

Note: * are the experimental data, obtained in the present work; α is the linear extension coefficient; K is the heat conductivity; n is the refractive index; D is the reduced focal power of the thermal lens; $\sigma_{ab/em}$ is the absorption/emission cross section; τ is the lifetime of the excited state; and λ_{em} is the radiation wavelength.

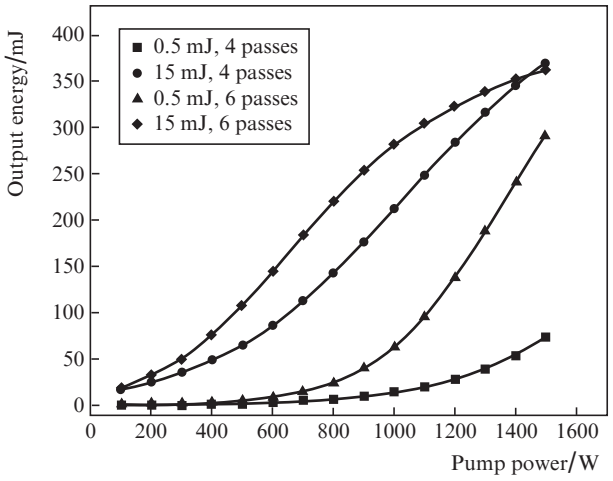

Figure 9. Dependences of the output energy of the radiation amplified by the second stage of the multipass amplifier on the pump power for 4 and 6 passes at the input energy E_{in} = 0.5 and 15 mJ (T = 80 K).

amplifier with the pump up to 1.5 kW at the initial energies of the amplified pulse 0.6 and 15 mJ, obtained in the first stage of amplification, at 300 and 80 K, respectively. The analysis was carried out for cryogenic temperatures of the active medium, the Yb:Y_2O_3 ceramics 1.5 mm thick, the diameters of the pump and signal beams being equal to 4 mm. From Fig. 9 it follows that the cryogenic regime of the two-step multipass amplifier allows an increase in the output energy up to 350 mJ, which is sufficient for implementing the terawatt stage of creating the multiterawatt femtosecond laser system operating at the kilohertz pulse repetition rate.

5. Conclusions

The components of a high-intensity solid-state laser system are developed, which can operate with a high pulse repetition rate under the condition of optical synchronisation of the channel of parametric amplification of femtosecond pulses in nonlinear optical crystals and the channel of pumping by the pulses of picosecond duration of parametric amplifiers with ytterbium-doped crystalline and ceramic active media, pumped by the radiation of laser diodes. The layouts of the optical schemes are developed and the calculations of a step-by-step increase in the output power in the amplification channel up to the subpetawatt level on the basis of parametric amplification in the LBO crystals with picosecond pumping are performed.

Using the created components in the pump channel of the laser system, the parameters of the preliminary amplifier of picosecond radiation with the output energy ~1 mJ at the wavelength 1030 nm with f = 1kHz are experimentally studied. The optimal optical scheme is developed for the multistage multipass cryogenic amplifier on the basis of Yb:Y_2O_3 laser ceramics pumped by the radiation from kilowatt diode lasers, aimed at achieving the output energy in the range 0.25–0.35 J. Experimental analysis of the peculiarities of operation of this scheme will be a subject of further studies.

Acknowledgements. The authors thank S.N. Bagayev for attention and support of this work and A.V. Kirpichnikov for help in the research.

This work was supported by the Presidium of the Russian Academy of Sciences in the framework of the Programme 'Extreme Light Fields and Their Applications' and the RF President's Programme of State Support to the Leading Scientific Schools (Grant No. NSh-4096.2014).

References

1. Korzhimanov A.V., Gonoskov A.A., Khazanov E.A., Sergeev A.M. *Usp. Fiz. Nauk*, **181** (1), 9 (2011) [*Phys. Usp.*, **54**, 9 (2011)].
2. http://www.extreme-light-infrastructure.eu/pictures/ELI-scientific-case-id17.pdf.
3. Major Z., Trushin S.A., Ahmad I., Siebold M., Wandt C., Klingebiel S., Wang T., Fülöp J.A., Henig A., Kruber S., Weingartner R., Popp A., Osterhoff J., Hörlein R., Hein J., Pervak V., Apolonski A., Krausz F., Karsch S. *Rev. Laser Eng.*, **37** (6), 431 (2009).
4. Chanteloup J.C., Albach D. *IEEE Photon.*, **3**, 245 (2011).
5. Mason P.D., Banerjee S., Ertel K., Phillips P.J., Greenhalgh J., Collier J.L. *Plasma Fusion Res.*, **8**, 3404051 (2013).
6. Divoky M., Sawicka M., Sikocinski P., Lucianetti A., Novak J., Rus B., Mocek T. *EPJ Web Conf.*, **59**, 08004 (2013).
7. Agrawal G. *Nonlinear Fibre Optics* (San Diego: Academic Press, 2001; Moscow: Mir, 1996).
8. Petrov V.V., Pestryakov E.V.,Trunov V.I., Kirpichnikov A.V., Merzlyakov M.A., Laptev A.V. *Opt. Atmos. Okean.*, **25** (3), 285 (2012).
9. Petrov V.V., Pestryakov E.V., Laptev A.V., Frolov S.A., Trunov V.I., Kirpichnikov A.V. *Techn. Dig. Intern. Conf. ICONO/LAT 2013* (Moscow, Russia, 2013) paper LWE5, p. 24.
10. Laptev A.V., Polyakov K.V., Petrov V.V., Pestryakov E.V. *Techn. Dig. XV Intern. Conf. Laser Optics* (St. Petersburg, Russia, 2012) paper YS_0521.
11. Sanghera J., Shaw B., Kim W., Villalobos G., Baker C., Frantz J., Hunt M., Sadowski B., Aggarwal I. *Proc. SPIE Int. Soc. Opt. Eng.*, **7912**, 79121Q-1 (2011).
12. Cardinali V., Marmois E., Le Garrec B., Bourdet G. *Opt. Mater.*, **34**, 990 (2012).
13. Beil K., Fredrich-Thornton S.T., Tellkamp F., Peters R., Kränkel C., Petermann K., Huber G. *Opt. Express*, **18** (20), 20712 (2010).
14. Peters V., *Growth and Spectroscopy of Ytterbium-doped Sesquioxides, Dissertation* (Hamburg: Institute für laser-physik, Universität Hamburg, 2011).
15. Cheng S., Xu X., Li D., Zhou D., Wua F., Zhao Z., Xu J. *Opt. Mater.*, **33**, 112 (2010).
16. Tso Yee Fan, Ripin D.J., Aggarwal R. *IEEE J. Sel. Top. Quantum Electron.*, **13** (3), 448 (2007).
17. Koechner W., Bass M. *Solid-State Lasers* (Oxford: Oxford Univ. Press, 2003) pp 137–198.
18. Pereverzentsev E.A., Mukhin I.B., Palashov O.V., Khazanov E.A. *Kvantovaya Elektron.*, **39** (9), 807 (2009) [*Quantum Electron.*, **39** (9), 807 (2009)].